Primary Frequency Support in Unit Commitment Using a Multi-Area Frequency Model with Flywheel Energy Storage

Salar Saberi Oskouee, Sadegh Kamali, and Turaj Amraee, *Senior Member, IEEE*

***Abstract*-- In this paper, a Frequency Stability Constrained Unit Commitment (FSCUC) model is presented. The on/off status of generating units, generation levels and operating reserves are optimized to minimize the operational daily costs. The frequency stability constraints are included in the proposed FSCUC model to guarantee the safety of System Frequency Response (SFR) under sudden generation outages. A new multi-area SFR model is proposed to capture the regional dynamics of system frequency with considering the impacts of transmission network. An SFR model is developed for each electric region and then the resulted regional SFRs are coupled via a set of constraints. In order to enhance the primary SFR and keep the daily operating point at its economic schedule, Flywheel Energy Storage (FES) devices are utilized in the proposed FSCUC model. The proposed multi-area SFR model allows the optimal allocation of operating reserve and the accurate modeling of FESs in FSCUC model. The proposed FSCUC model is formulated as a Mixed Integer Linear Programming (MILP) problem and is applied over the IEEE 118-bus test system to show the accuracy of the proposed multi-region SFR and the impact of FES in frequency support. The developed MILP model is solved using CPLEX in GAMS.**

***Index Terms*— Unit Commitment, Primary Frequency Response, Frequency Nadir, Flywheel, Optimization.**

NOMENCLATURE

Indices and Sets

i, j	Indices of all buses
c, d	Indices of electric areas
t, τ	Indices of time intervals
k	Index of PWL segments
n	Index of time steps in frequency response
v	Index of generation outages
Ω_B, Ω_G	Sets of all buses, generators
Ω_L, Ω_A	Sets of transmission lines, electric areas
Ω_N	Set of time steps in frequency response
Ω_T	Set of time intervals (i.e. 24 hours)
Ω_K	Set of segments in linearized cost function
Ω_C^B, Ω_C^G	Sets of buses and generators in area c
Ω_C^{Go}	Set of governors in area c
Ω_C^F	Set of outages in area c
Ω_{LA}	Set of transmission lines between areas

Authors are with the Faculty of the Electrical Engineering, K.N.Toosi University of Technology, Tehran (14317-14191), Iran.

Parameters

C_i^{Pmin}	Generation cost of unit i at minimum generation
C_i^{SD}, C_i^{SU}	Shut down cost, Start-up cost of unit i
$C_{i,k}^{PG}$	Generation cost of unit i in linearized k^{th} segment
$P_{i,t}^D$	Demand power of bus i at scheduling hour t
$B_{i,j}$	Suseptance of line between bus i to j
$B_{c,d}^a$	Equivalent Suseptance between area c to d
$B_{c,t}^{eq}$	Equivalent Suseptance for c^{th} area at hour t
$B_{c,t}^{eqtr}$	Transient equivalent suseptance of c^{th} area at hour t
$P_{i,j}^{Lmax}$	Maximum power flow across line $i\ to\ j$
P_i^{min}	Minimum power generation of unit i
P_i^{max}	Maximum power generation of unit i
MU_i, MD_i	Minimum up and down times of unit i
RU_i, RD_i	Ramp up and ramp down rates of unit i
Res_c	The amount of system required reserve at area c
S_i	Base apparent power of unit i
H_i	Inertia time constant of unit i
R_i	Governor droop of unit i
R_c^{FL}	Droop of the flywheel at area c
E_c^{FLmax}	Maximum energy of the flywheel at area c
E_c^{FLmin}	Minimum energy of the flywheel at area c
NT	Number of time intervals (i.e. 24 hours)
NK	Number of PWL segments
M	A large positive number
Δt	Time step of SFR discretization
Fs	Network frequency
$Fm_{v,c}$	An identity diagonal matrix in SFR model (1 if fault v occurs in area c and 0 otherwise)
$Tl_{c,d}$	A matrix for coincidence of transmission lines and areas (1 if area c is connected to line d and 0 otherwise)
F_{nadir}	Nadir or minimum point of frequency response
Δfss^{max}	Maximum steady state frequency deviation from Fs
TK	Time constant of governors
DF	Load damping factor

Variables

$U_{i,t}$	Binary variable for unit i status at hour t (1 if unit is on and 0 otherwise)
$\varphi_{i,t}$	Binary variable ,1 if unit i is on at hour t and was on at hour $t-1$

$\alpha_{i,t}$	Binary variable ,1 if unit i at hour t turns on and 0 otherwise
$\beta_{i,t}$	Binary variable ,1 if unit i at hour t turns off and 0 otherwise
$U^{O}_{v,i,t}$	Binary variable ,0 if unit i under fault v at hour t is disconnect from the network and 1 otherwise
$U^{F}_{v,i,t}$	Binary variable ,1 if unit i at hour t is on during fault and 0 otherwise
F_{Tot}	Total generation cost over the daily horizon
$P^{g}_{i,t}$	Power generation of unit i at hour t
$P^{gk}_{i,k,t}$	Power generation of unit i at k^{th} segment and hour t
$P^{ga}_{c,t}$	Equivalent power generation of area c at hour t
$P^{Da}_{c,t}$	Equivalent demand of area c at hour t
$PL_{i,j,t}$	Power flow from bus $i\ to\ j$ at hour t
$PL^{a}_{c,d,t}$	Power flow from area $c\ to\ d$ at hour t
$\theta_{i,t}$	Voltage angle for bus i at hour t
$\theta^{a}_{c,t}$	Equivalent voltage angle of area c at hour t
$\theta^{af}_{v,c,t,n}$	Equivalent voltage angle of area c during fault v at hour t and n^{th} time step
$\Delta P_{c,t}$	Generation outage in area c at hour t
$\Delta P^{e}_{v,c,t}$	Electrical power differences in area c under fault v at hour t for swing equation
$\Delta P^{pu}_{v,c,t}$	Per-unit lost power in area c under fault v at hour t
$\delta_{c,t}$	Equivalent rotor angle of area c at hour t
$\delta^{f}_{v,c,t}$	Equivalent rotor angle of area c under fault v at hour t for swing equation
$\delta^{f}_{v,c,t,n}$	Equivalent rotor angle of area c under fault v at hour t and n^{th}time step
$PL^{af}_{v,c,d,t,n}$	Power flow from area $c\ to\ d$ under fault v at hour t and n^{th} time step
$PL^{afpu}_{v,c,t,n}$	Per-Unit power flow from area c under fault v at hour t and n^{th} time step
$H^{eq}_{v,c,t}$	Equivalent inertia constant of area c under fault v at hour t
$R^{eq}_{v,c,t}$	Equivalent governor droop of area c under fault v at hour t
$f_{v,c,t,n}$	Frequency of area c during fault v at hour t and n^{th} time step
$\Delta f_{v,c,t,n}$	Frequency deviation of area c from Fs under fault v at hour t and n^{th} time step
$f^{ss}_{v,t}$	Steady state frequency after fault v at hour t
$\Delta f^{ss}_{v,t}$	Steady state frequency deviation from Fs after fault v at hour t
$\Delta r_{v,c,t,n}$	Governor response in area c under fault v at hour t and n^{th} time step
$\Delta P^{FL}_{v,c,t,n}$	Power difference for the flywheel in area c under fault v at hour t and n^{th} time step
$E^{FL}_{v,c,t,n}$	State of energy for the flywheel in area c under fault v at hour t and n^{th} time step
$A_{\{*\}}$	Auxiliary variable utilized for SFR linearization

I. Introduction

Proper tools should be taken into account to improve the stability in short term power system operational studies such as Unit Commitment (UC). The aim of UC is to determine the on/off status of generating units, their generation levels and the required reserves in a daily or weekly horizon [1]. Different technical constraints of generating units and transmission network are considered in UC problem [2]. The unit scheduling obtained by the UC problem impacts the system stability significantly. Among stability phenomenon, the transient stability and frequency stability are highly affected. In [3]-[4], the transient stability has been included in the UC problem using the decomposition techniques, in which the transient stability is assessed via proper sub-problems. Also, due to the computational complexity, in [3], the Real Time Digital Simulators (RTDS) have been utilized. Also, in [5], a Transient Stability Constrained UC (TSCUC) model is presented using the transient energy function method. The transient energy function method used in [5], results in efficient assessment of transient stability in a separate sub-problem. Frequency stability is another important stability phenomenon that is needed to be considered in the Economic Dispatch (ED), Optimal Power Flow (OPF) and UC studies. In [6], a joint model that co-optimizes both slow timescale ED resources and fast frequency regulation resources has been proposed. The same study using the model predictive algorithm is proposed in [7] for optimal load frequency control to co-optimize the frequency regulation and ED problem. In [8], an OPF model is presented for generation re-dispatch considering dynamic frequency response constraints. The proposed frequency stability OPF model is formulated as a set of differential algebraic equations (DAEs). In frequency stability constrained ED and OPF models, the on/off states of generating units are assumed to be known. However, the on/off states of generating units along with the power generation levels impacts the frequency stability. Therefore, including frequency stability constraints in UC study is a prerequisite to reach a stable daily unit scheduling. Conventionally, a predetermined amount of operating reserve is considered in UC model to handle the forced generation outages [9]. The contingency reserve should be fast enough to keep the system frequency within a safe range, when the outage of a main generating unit results in generation deficiency [10]-[11]. Without fast and enough operating reserves, the abnormal frequency nadirs are expected and may result in load shedding or generation trip due to the activation of under frequency relays. However, large amount of contingency reserve imposes additional cost to the UC problem [12]. In [13], a Modified Interval Unit Commitment (MIUC) model is proposed to minimize the generation scheduling cost and optimize the primary frequency response including Rate-of-Change-of-Frequency (RoCoF), frequency nadir (i.e. the minimum point in system frequency response) and steady state frequency under wind penetration. In [14], a mixed integer linear programming (MILP) formulation is presented for stochastic unit commitment to optimize energy production, spinning reserves, and inertia-dependent fast frequency response under wind uncertainty and generation outages. In [13]-[14], the system frequency response is formulated using the Center-of-Inertia (COI) or single bus mode. In [15], the primary frequency response is included in the Security-Constrained Unit Commitment (SCUC) problem and based on the low-order frequency response model proposed in [16], the sensitivity of the frequency drop to the governor parameters is

extracted. In [17], an UC model is proposed for scheduling the reserve requirement for primary frequency regulation considering only a quasi-steady-state frequency limit. In [18], a stochastic UC model is proposed to co-optimize the energy production and the inertia and primary frequency response, supporting the frequency-nadir. In [13]-[18], the system frequency response is considered using an equivalent SFR model without considering the local dynamics of frequency dynamics. Also, in [13]-[18], the frequency stability is provided by adjusting unit scheduling that deviates the operating point from its economic schedule. Recently, to preserve the system frequency stability under high shares of renewable resources, new control strategy is designed for inertia-free renewable resources. In [19], a variable virtual inertia control strategy is presented for the frequency constrained UC model. In [19], the rate of change of frequency and frequency nadir are analytically considered as the frequency constraints. Another frequency stability constrained UC model is proposed in [20], where the analytical system frequency constraints with virtual inertia from wind turbines are incorporated into a stochastic UC model. In [21], the maximum power imbalance that the system can tolerate without violating frequency limits is defined as the frequency stability margin. The frequency nadir is analytically determined using a linearized model and is then added to the UC model. Both the thermal generators and the variable renewable energy resources are considered as the frequency support tools.

Utility scale Energy Storage Systems (ESSs) have been utilized for different purposes in UC studies [22]. Large scale and fast response ESS can contribute in inertial and primary frequency response [23]. In [24], fast-response battery energy storages are utilized in a frequency stability constrained UC model to maintain the frequency response under generation outages. Flywheel energy storage (FES) is a powerful ESS that can be used for primary frequency support. The impacts of FES on system stability is investigated in [25]. In [26]and [27], efficient models are proposed for Flywheel as a short term energy storage. Conventionally, the frequency stability constraints are not considered in the UC model. However, after obtaining the daily unit commitment plan, the frequency stability of the system is checked by proper dynamic stability simulators. The UC models are inherently very complicated problems and by adding the discretized equations of system frequency model to the UC, the computational complexity will be increased significantly. Using proper SFR models, the frequency stability constrained UC models can be realized provided that there are powerful computational tools.

Regarding previous frequency stability constrained unit scheduling models, there are still some major gaps that should be addressed. In previous proposed approaches, the system frequency response is considered using an equivalent SFR model relying on the COI concept without considering the local dynamics of frequency response. The single or equivalent SFR based UC models will not guarantee the safety of system frequency response especially in multi-area power systems. Additionally, in previous proposed frequency constrained UC models, no effort has been made to include the FES as an inertia frequency support measure. Regarding these gaps, the main contributions of this paper are as follows:

- Proposing a Frequency Stability Constrained UC (FSCUC) model to optimize the unit scheduling, operating reserves, and primary frequency response under generation outages. The FES is utilized as the inertial frequency support device that can minimize the additional costs imposed by frequency stability constraints in FSCUC model. In addition to the conventional frequency supporting tools, the FES is formulated and integrated in the proposed FSCUC model to preserve the frequency stability while the generating units are scheduled in their most economic loading pattern.
- A multi-area SFR model is proposed to capture the regional characteristics of frequency dynamics. Unlike the equivalent COI SFR models (i.e. single SFR models), the proposed regional SFR considers the local variations of frequency dynamics. Regarding transmission network, coupling constraints are proposed to capture the frequency interactions between areas. The proposed multi-area SFR is able to consider the dynamics of Primary Frequency Control.
- Converting the proposed FSCUC model into an MILP optimization model to find the optimal unit scheduling, reserve allocation, and frequency support. The proposed multi-area SFR model is discretized in time and is added to the original UC model to find the most economic unit scheduling with sufficient frequency stability support tools.

The rest of this paper is organized as follows. The formulation of the proposed UC model including the detailed formulations of the proposed multi-area SFR model and the FES are given in Section II. The simulation results of the proposed method over the dynamic IEEE 118-bus test system is presented in Section III. Finally, the major findings of this research are given in Section IV.

II. Model Formulation

The objective function of the UC problem is defined to minimize the generation cost, start up and shut down costs of thermal generating units. Different constraints including units' constraints (e.g. minimum/maximum generation limits, minimum up and down times, ramp up and down rates) and the network constraints (i.e. reserve requirement, and power flow limits) are considered [1]. Using the Piece Wise Linear (PWL) technique, the quadratic objective function of the UC problem is linearized to minimize the total operation cost of thermal units as follows:

$$Min\ F_{Tot} = \sum_{t\in\Omega_T}\sum_{i\in\Omega_G}\left[C_i^{Pmin} * U_{i,t} + \alpha_{i,t} * C_i^{SU} + \beta_{i,t} * C_i^{SD} + \left(\sum_{K\in\Omega_K} C_{i,k}^{PG} * P_{i,k,t}^{gk}\right)\right] \quad (1)$$

Power generation of each unit consists of minimum generation power of a unit plus the total power generations of all linearized segments as given by (2).

$$P_{i,t}^{g} = P_i^{min} * U_{i,t} + \sum_{k\in\Omega_K} P_{i,k,t}^{gk} \qquad \forall\, i\in\Omega_G\,, t\in\Omega_T \quad (2)$$

A. Constraints of Unit commitment

Due to the nonlinearity and complexity of AC power flow model, DC power flow is utilized to check the power balance and the power flows of transmission lines. Power balance and power flow constraints are considered as given by (3) and (4), respectively.

$$P_{i,t}^{g} = \sum_{i,j \in \Omega_L} PL_{i,j,t} + P_{i,t}^{D} \qquad \forall\, i,j \in \Omega_B\,, t \in \Omega_T \qquad (3)$$

$$PL_{i,j,t} = B_{i,j} * (\theta_{i,t} - \theta_{j,t}) \qquad \forall i,j \in \Omega_L, t \in \Omega_T \qquad (4)$$

The transmission flows are constrained as follows:

$$-P_{i,j}^{Lmax} \le P_{i,j,t}^{L} \le P_{i,j}^{Lmax} \qquad \forall i,j \in \Omega_L\,, t \in \Omega_T \qquad (5)$$

In order to handle the single generation outages, a minimum amount of spinning reserve is required to be allocated as the contingency reserve. The reserve constraint is satisfied according to (6).

$$\sum_{i \in \Omega_C^G} (P_i^{max} * U_{i,t}) \ge (1 + Res_c) * \sum_{i \in \Omega_C^G} P_{i,t}^{D} \qquad \forall\, c \in \Omega_A\,, t \in \Omega_T \qquad (6)$$

Generation level of each unit is limited according to (7). Since the cost function is linearized using the PWL technique, the power generation of each linearized segment is constrained based on (8).

$$P_i^{min} * U_{i,t} \le P_{i,t}^{g} \le P_i^{max} * U_{i,t} \qquad \forall i \in \Omega_G\,, t \in \Omega_T \qquad (7)$$

$$0 \le P_{i,k,t}^{gk} \le [(P_i^{max} - P_i^{min})/NK] * U_{i,t} \qquad \forall i \in \Omega_G\,, k \in \Omega_K, t \in \Omega_T \qquad (8)$$

According to (9)-(13), the minimum up and minimum down times of generating units are satisfied [28]-[29].

$$\alpha_{i,t} - \beta_{i,t} = U_{i,t} - U_{i,t-1} \qquad \forall i \in \Omega_G\,, t \in \Omega_T \qquad (9)$$

$$\sum_{t=\tau}^{t+MU_i-1} U_{i,t} \ge \alpha_{i,t} * MU_i \qquad (10)$$

$$\forall i \in \Omega_G\,, t = 1, \dots, NT - MU_i + 1$$

$$\sum_{t=\tau}^{NT} U_{i,t} \ge \alpha_{i,t} * (NT - t + 1) \qquad (11)$$

$$\forall i \in \Omega_G\,, t = NT - MU_i + 2, \dots, NT$$

$$\sum_{t=\tau}^{t+MD_i-1} [1 - U_{i,t}] \ge \beta_{i,t} * MD_i \qquad (12)$$

$$\forall i \in \Omega_G\,, t = 1, \dots, NT - MD_i + 1$$

$$\sum_{t=\tau}^{NT} [1 - U_{i,t}] \ge \beta_{i,t} * (NT - t + 1) \qquad (13)$$

$$\forall i \in \Omega_G\,, t = NT - MD_i + 2, \dots, NT$$

Ramp up and down rates of each unit are considered based on (14) and (15), respectively. These nonlinear constraints are linearized as given in Part A of the Appendix.

$$P_{i,t}^{g} - P_{i,t-1}^{g} \le (1 - U_{i,t-1}) * U_{i,t} * P_i^{min} + RU_i * [U_{i,t} * (U_{i,t-1} - 1)] \qquad (14)$$

$$\forall i \in \Omega_G\,, t \in \Omega_T$$

$$P_{i,t-1}^{g} - P_{i,t}^{g} \le (1 - U_{i,t}) * U_{i,t-1} * P_i^{min} + RD_i * [U_{i,t-1} * (U_{i,t} - 1)] \qquad (15)$$

$$\forall i \in \Omega_G\,, t \in \Omega_T$$

B. Proposed Multi-Area System Frequency Response

Conventionally, in frequency stability constrained UC models, a single bus SFR model such as COI frequency model is utilized [15]- [16]. In large scale or multi-area power systems, a single SFR is not enough to represent the frequency dynamics of regions. In fact, a generation outage in a given electric area causes different SFR with different frequency nadirs in all regions, and a single equivalent SFR is not able to capture the local changes of system frequency. Therefore, to represent the frequency stability in UC study, an accurate multi-area SFR model is required. Additionally, a multi-area SFR model allows the accurate and efficient utilization of FES in primary frequency support.

The aim of the proposed FSCUC model is to optimize the unit scheduling and frequency stability under single outages of largest generating unit in each area according to (16)-(19). Indeed, the outage of the largest generating unit is interpreted as the generation deficiency or the input disturbance in SFR model.

$$\Delta P_{c,t} \ge P_{i,t}^{g} \qquad \forall i \in \Omega_C^G, c \in \Omega_A, t \in \Omega_T \qquad (16)$$

$$-M * (\Delta P_{c,t} - P_{i,t}^{g}) \le U_{v,i,t}^{O} \qquad \forall i \in \Omega_C^G, c \in \Omega_A, t \in \Omega_T \qquad (17)$$

$$U_{v,i,t}^{O} \le M * (\Delta P_{c,t} - P_{i,t}^{g}) \qquad \forall i \in \Omega_C^G, c \in \Omega_A, t \in \Omega_T \qquad (18)$$

$$\Delta P_{c,t} - P_{i,t}^{g} \le M * U_{v,i,t}^{O} \qquad \forall i \in \Omega_C^G, c \in \Omega_A, t \in \Omega_T \qquad (19)$$

Using (16), the amount of maximum generation level is stored in $\Delta P_{c,t}$ variable that is defined as the generation deficiency and will be used in proposed System Frequency Response as the input disturbance. However, this is not enough, and we need to determine the number (i.e. bus number) of the generator with the maximum generation level to be multiplied by $U_{v,i,t}^{O}$. So the developed program checks if a unit is the generators with maximum generation level. If the i^{th} unit is the unit with maximum generation level, then $\Delta P_{c,t} = P_{i,t}^{g}$, and according to (17) -(19), $U_{v,i,t}^{O} = 0$, otherwise if the i^{th} unit is not the unit with maximum generation level, then $\Delta P_{c,t} \ne P_{i,t}^{g}$, and according to (17) -(19), $U_{v,i,t}^{O} = 1$. The output of (16) -(19) will be used in (21) -(22).

Since the frequency response depends on the system inertia, it is required to determine the on/off status of generating units based on (20)-(24). Indeed, the constraints given in (20)-(24) couples the SFR model with the UC model.

$$U_{v,i,t}^{F} \le U_{i,t} \qquad \forall i \in \Omega_C^G, v \in \Omega_C^F, t \in \Omega_T \qquad (20)$$

$$U_{v,i,t}^{F} \le U_{v,i,t}^{O} \qquad \forall i \in \Omega_C^G, v \in \Omega_C^F, t \in \Omega_T \qquad (21)$$

$$U_{v,i,t}^{F} \ge U_{i,t} + U_{v,i,t}^{O} - 1 \qquad \forall i \in \Omega_C^G, v \in \Omega_C^F, t \in \Omega_T \qquad (22)$$

$$\sum_{i \in \Omega_C^G} U_{v,i,t}^{F} = \left(\sum_{i \in \Omega_C^G} U_{i,t} \right) - 1 \qquad (23)$$

$$\forall i \in \Omega_C^G, v \in \Omega_C^F, t \in \Omega_T \text{ and } \forall i \in \Omega_k^G, v \in \Omega_k^F, k = [1,2,3]$$

$$U_{v,i,t}^{F} = U_{i,t} \qquad (24)$$

$$\forall i \in \Omega_C^G, v \in \Omega_C^F, t \in \Omega_T \text{ and } \forall i \in \Omega_k^G, v \notin \Omega_k^F, k = [1,2,3]$$

In order to have a specific SFR for each region, first the total generation and load of each electric area are determined based on (25) and (26), respectively.

$$P_{c,t}^{ga} = \sum_{i \in \Omega_C^G} P_{i,t}^{g} \qquad \forall c \in \Omega_A, t \in \Omega_T \qquad (25)$$

$$P_{c,t}^{Da} = \sum_{i \in \Omega_C^G} P_{i,t}^{D} \qquad \forall c \in \Omega_A, t \in \Omega_T \qquad (26)$$

Now, it is required to couple the power flow model between electric areas. The constraints given in (27) and (28) represent the power balance and dc power flow between electric areas. In this paper, the proposed SFR is a multi-area formulation and is extracted based on the equivalent rotor angles of equivalent generators in each region. Each region is represented with an equivalent generator. According to (29), the rotor angle for the equivalent generator of the c^{th} area at hour t is determined.

$$P_{c,t}^{ga} + \sum_{c,d \in \Omega_{LA}} PL_{c,d,t}^{a} = P_{c,t}^{Da} \qquad \forall c \in \Omega_A, t \in \Omega_T \qquad (27)$$

$$PL_{c,d,t}^{a} = B_{c,d}^{a} * (\theta_{c,t}^{a} - \theta_{d,t}^{a}) \qquad \forall c,d \in \Omega_A, t \in \Omega_T \qquad (28)$$

$$P_{c,t}^{ga} = B_{c,t}^{eq} * (\delta_{c,t} - \theta_{c,t}^{a}) \qquad \forall c \in \Omega_A, t \in \Omega_T \qquad (29)$$

The constraints given in (27)-(29), refer to the steady state power flow during the scheduling horizon (i.e. t=1,…,24).

Therefore the variables of $\theta^{a}_{c,t}$ and $\delta_{c,t}$ are the steady state variables in power flow of the UC model. The variables of $\theta^{af}_{v,c,t,n}$ and $\delta^{f}_{v,c,t,n}$ are the dynamic variables used in SFR discretized frequency model. The initial values of $\theta^{af}_{v,c,t,n}$ and $\delta^{f}_{v,c,t,n}$ are assumed as $\theta^{a}_{c,t}$ and $\delta_{c,t}$ according to (30) and (31), respectively. Note that the index of *t* represents the hourly time intervals of daily unit scheduling, while the time variation of SFR in each hour is represented by *n*.

$$\theta^{af}_{v,c,t,n} = \theta^{a}_{c,t} \qquad \forall v \in \Omega^{F}_{C}, c \in \Omega_{A}, t \in \Omega_{T}, n = 1 \quad (30)$$

$$\delta^{f}_{v,c,t,n} = \delta_{c,t} \qquad \forall v \in \Omega^{F}_{C}, c \in \Omega_{A}, t \in \Omega_{T}, n = 1 \quad (31)$$

The constraints (32) and (33) represent the power balance and dc power flow between equivalent areas during generation outage. The generation outage is assumed as the input disturbance or input fault that governs the frequency dynamics or SFR. Therefore, the changes of rotor angles and voltage magnitudes in electric areas is caused by the power imbalance. The power balance in each electric area is satisfied using (32). According to (32), the power flow from area c to d under fault v at hour t and n^{th} time step is related to the generation deficiency or generation outage at that area and the resulted change in electric power output of the equivalent generators of the area. Also, the power flow between electric areas is represented using (33). The relation between the frequency and rotor angle of each area is expressed by (34).

$$PL^{af}_{v,c,d,t,n} = Tl_{c,d} * [-Fm_{v,c} * \Delta P_{c,t} + B^{eqtr}_{c,t} * [(\delta^{f}_{v,c,t,n} - \delta_{c,t}) - (\theta^{af}_{v,c,t,n} - \theta^{a}_{c,t})] \quad (32)$$
$$\forall v \in \Omega^{F}_{C}, (c,d) \in \Omega_{A}, t \in \Omega_{T}, n \in \Omega_{N}$$

$$PL^{af}_{v,c,d,t,n} = B^{a}_{c,d} * [(\theta^{af}_{v,c,t,n} - \theta^{a}_{c,t}) - (\theta^{af}_{v,d,t,n} - \theta^{a}_{d,t})] \quad (33)$$
$$\forall v \in \Omega^{F}_{C}, (c,d) \in \Omega_{A}, t \in \Omega_{T}, n \in \Omega_{N}$$

$$\left[\frac{\delta^{f}_{v,c,t,n} - \delta^{f}_{v,c,t,n-1}}{\Delta t}\right] = 2\pi * (\frac{f_{v,c,t,n}}{Fs}) \quad (34)$$
$$\forall v \in \Omega^{F}_{C}, c \in \Omega_{A}, t \in \Omega_{T}, n \in \Omega_{N}$$

The amount of generation outage and power flow during each disturbance in each area is expressed in per-unit as given in (35) and (36).

$$\Delta P^{pu}_{v,c,t} = Fm_{v,c} * \frac{\Delta P_{c,t}}{\sum_{i \in \Omega_{G}} S_{i} * U^{F}_{v,i,t}} \qquad \forall v \in \Omega^{F}_{C}, c \in \Omega_{A}, t \in \Omega_{T} \quad (35)$$

$$PL^{afpu}_{v,c,t,n} = \frac{\sum_{d \in \Omega_{A}} Tl_{c,d} * PL^{af}_{v,c,d,t,n}}{\sum_{i \in \Omega_{G}} S_{i} * U^{F}_{v,i,t}} \quad (36)$$
$$\forall v \in \Omega^{F}_{C}, c \in \Omega_{A}, t \in \Omega_{T}, n \in \Omega_{N}$$

The equivalent inertia constant and governor droop of each area are determined using (37) and (38), respectively.

$$H^{eq}_{v,c,t} = \frac{\sum_{i \in \Omega^{G}_{C}} H_{i} * S_{i} * U^{F}_{v,i,t}}{\sum_{i \in \Omega_{G}} S_{i} * U^{F}_{v,i,t}} \qquad \forall v \in \Omega^{F}_{C}, c \in \Omega_{A} \quad (37)$$

$$\frac{1}{R^{eq}_{v,c,t}} = \frac{\sum_{i \in \Omega^{Go}_{C}} \frac{S_{i} * U^{F}_{v,i,t}}{R_{i}}}{\sum_{i \in \Omega_{G}} S_{i} * U^{F}_{v,i,t}} \qquad \forall v \in \Omega^{F}_{C}, c \in \Omega_{A} \quad (38)$$

The swing equation for the proposed multi-region SFR is considered as given in (39). The dynamics of governors, load damping, exchanged power between regions and the FES are included in the proposed multi-region SFR. The discretized swing equation is reformulated as given in (40).

$$\frac{d^{2}\delta^{f}_{v,c,t}}{dt^{2}} = \frac{-\Delta P^{e}_{v,c,t}}{2H^{eq}_{v,c,t}} \qquad \forall v \in \Omega^{F}_{C}, c \in \Omega_{A}, t \in \Omega_{T} \quad (39)$$

$$\frac{\Delta f_{v,c,t,n} - \Delta f_{v,c,t,n-1}}{\Delta t} = \frac{1}{2H^{eq}_{v,c,t}} * (\Delta r_{v,c,t,n} - \Delta P^{pu}_{v,c,t} - PL^{afpu}_{v,c,t,n+1} - \Delta P^{FL}_{v,c,t,n} - DF/3 * \Delta f_{v,c,t,n}) \quad (40)$$
$$\forall v \in \Omega^{F}_{C}, c \in \Omega_{A}, t \in \Omega_{T}, n \in \Omega_{N}$$

Now, the proposed discretized SFR is introduced as given in (41)-(45). A major requirement in FSCUC model is to keep the frequency nadir within a safe range. To this end, the constraint given in (45) is introduced to avoid the undesired frequency nadirs in SFR. According to the operational rules, the frequency nadir should remain above the threshold of Under Frequency Load Shedding (UFLS) relays to avoid any automatic load shedding. The frequency set-point of the first stage of UFLS relays are not activated for frequency changes within $\pm 0.5Hz$. Indeed, all synchronous generators can withstand frequency deviation within $\pm 0.5Hz$. Regarding these issues, in this paper, the limit of frequency nadir is set at 49.5 Hz.

$$f_{v,c,t,n} = Fs * (1 + \Delta f_{v,c,t,n}) \qquad \forall v \in \Omega^{F}_{C}, c \in \Omega_{A}, t \in \Omega_{T}, n \in \Omega_{N} \quad (41)$$

$$\Delta f_{v,c,t,n} = \Delta f_{v,c,t,n-1} + A_{v,c,t,n-1} * \Delta t \quad (42)$$
$$\forall v \in \Omega^{F}_{C}, c \in \Omega_{A}, t \in \Omega_{T}, n \in \Omega_{N}, n > 1$$

$$A_{v,c,t,n} = \frac{1}{2H^{eq}_{v,c,t}} * (\Delta r_{v,c,t,n} - \Delta P^{pu}_{v,c,t} - PL^{afpu}_{v,c,t,n+1} - \Delta P^{FL}_{v,c,t,n} - DF/3 * \Delta f_{v,c,t,n}) \quad (43)$$
$$\forall v \in \Omega^{F}_{C}, c \in \Omega_{A}, t \in \Omega_{T}, n \in \Omega_{N}$$

$$\Delta r_{v,c,t,n} = \Delta r_{v,c,t,n-1} + \frac{\Delta t}{TK} * ((-\Delta f_{v,c,t,n-1}/R^{eq}_{v,c,t}) - \Delta r_{v,c,t,n-1}) \quad (44)$$
$$\forall v \in \Omega^{F}_{C}, c \in \Omega_{A}, t \in \Omega_{T}, n \in \Omega_{N}, n > 1$$

$$f_{v,c,t,n} \geq F_{nadir} \qquad \forall v \in \Omega^{F}_{C}, c \in \Omega_{A}, t \in \Omega_{T}, n \in \Omega_{N} \quad (45)$$

The primary frequency stability support can be achieved using different tools such as Energy Storage (ES) devices. In this paper, FES device is utilized for frequency support or inertial frequency response in UC study, due to its fast response, very low energy loss, and high reliability with respect to other ES types such as BES systems. Also, practical FES systems around the world are growing. For example, 40MW of flywheel energy storage is already in operation in grid-balancing markets for frequency support in New York State and Pennsylvania [30]. The contribution of FES in primary frequency response is determined based on the system frequency deviation and FES characteristics. Power difference and state of energy for a given FES in area c during each disturbance (i.e. generation deficiency represented by $\Delta P^{pu}_{v,c,t}$) are considered according to (46) and (47), respectively.

$$\Delta P^{FL}_{v,c,t,n} = \Delta f_{v,c,t,n}/R^{FL}_{c} \qquad \forall v \in \Omega^{F}_{C}, c \in \Omega_{A}, t \in \Omega_{T}, n \in \Omega_{N} \quad (46)$$

$$E^{FL}_{v,c,t,n} = E^{FL}_{v,c,t,n-1} + \Delta P^{FL}_{v,c,t,n} * \Delta t \quad (47)$$
$$\forall v \in \Omega^{F}_{C}, c \in \Omega_{A}, t \in \Omega_{T}, n \in \Omega_{N}., n > 1$$

The nonlinear constraints given by (35)-(38), (43)-(44), and (46) are linearized as given in Part B of the Appendix. Quasi steady state frequency of the system under each disturbance is obtained according to (48) and (49). Additionally, the amount of quasi steady state frequency in all areas are the same and should be restored to a given threshold according to the constraint given by (50). The nonlinear constraint given by (48) is linearized as given in Part C of the Appendix.

$$\Delta f^{ss}_{v,t} = -\frac{\Delta P^{pu}_{v,c,t}}{DF + \frac{1}{R^{eq}_{v,c,t}}} \qquad \forall v \in \Omega^{F}_{C}, c \in \Omega_{A}, c = v, t \in \Omega_{T} \quad (48)$$

$$f^{ss}_{v,t} = Fs * (1 + \Delta f^{ss}_{v,t}) \qquad \forall v \in \Omega^{F}_{C}, t \in \Omega_{T} \quad (49)$$

$$-\Delta fss^{max} \leq \Delta f^{ss}_{v,t} \leq \Delta fss^{max} \qquad \forall v \in \Omega^{F}_{C}, t \in \Omega_{T} \quad (50)$$

III. CASE STUDY

IEEE 118-bus test system is used to verify the efficacy of the proposed FSCUC model. This test system includes 186 transmission lines, 64 PQ buses, and 54 PV nodes. The data of this test system are reported in [31]. Three areas are assumed

for IEEE-118 bus test system [32]. Power reserve for each area is considered to be 10 percent of the total load in each hour. The inertia and governor droops have been reported in Table I. Alternatively, all data can be found in [33]. By selecting the small time steps the accuracy of the obtained frequency response is promoted, however, the number of discretized samples is increased, and the computation time is increased. Beyond a given time step or Δt the accuracy of the obtained frequency response will not change, significantly. Regarding this issue, we have assumed $\Delta t = 0.1s$. The simulation results are presented in four different cases. In Case 1, the conventional network constrained UC model without considering frequency stability is applied to the test system. In Case 2, the efficacy of the conventional single bus SFR model is compared with the proposed multi-area SFR model under the unit scheduling obtained in case 1. In case 2-A, single SFR with frequency constraints is added to the UC problem and the results of the single SFR FSCUC model are discussed. In Case 3, the new proposed multi-area SFR model is included in the UC model and the results of the proposed FSCUC model are presented. In Case 4, the results of the proposed FSCUC model are given in the presence of the FES as a major source of inertial frequency support. Finally, in case 4-A, the performance of the flywheel-based FSCUC in low inertia condition is investigated. All MILP models of the UC and FSCUC models are solved using CPLEX in GAMS.

Table I
Dynamic Characteristics of Generating Units

Unit	H (s)	R(p.u)	Rated Power (MVA)
1,9,12,31,32	5.016	0	25
2,6,8,14,15,16,22,23,26,33, 34,35,37,38,43,47,48,50	1.2	0	25
3,42,49	4.4893	0	35.29
4,29,36	2.319	0.0085	590
5	4.768	0.04	125
7,30	1.52	0	40
10,20,45	3.006	0.0152	330
11	3.704	0.0122	410
13,19,39	6.187	0.066	75
17,53	5.078	0	51.2
18,44	6.186	0	75
21,46,51	4.985	0.05	100
24,25	4.122	0.0214	233
27,28	2.631	0.0098	512
40	2.6419	0.006	835
41,52	4.985	0	100
54	2.621	0	384

Case 1: Conventional Network Constrained UC Model

In this case, the network constrained UC model is simulated without considering the frequency stability constraints. All steady state unit and network constraints are included. The obtained results including On/Off states of units are reported in Table II. Total daily cost of unit scheduling is 818332.64$.

Case 2: Single SFR Versus Regional SFR

In previous proposed FSCUC models, the SFR was considered using a single equivalent SFR for the system. Under a given fault (i.e. generation outage), it is not realistic to assume a unique SFR model for the entire system. Therefore, in this case, the difference between the single SFR and the proposed multi-area SFR is shown under the unit scheduling obtained in Case 1. The aim of this case is to show just the difference between the single SFR model and the proposed multi-area SFR model. Note that, in this case, the SFR is not included in the optimization model of UC and this task is done in next cases. The largest generating units in each hour of the planning horizon is removed and the frequency responses are calculated using the single SFR and the multi-area SFR models. The power outage and the resulted frequency nadirs at each hour are given in Table III. For the single SFR, at each hour, one equivalent SFR is obtained while using the multi-area SFR, three frequency responses are obtained for each area at each hour.

Table II
The On /Off States of Generating Units in Case 1

Unit	Hours (1-24)
1-3	0 0 0 0 0 0 0 0 0 0 0 0 0 0 0 0 0 0 0 0 0 0 0 0
4-5	1 1 1 1 1 1 1 1 1 1 1 1 1 1 1 1 1 1 1 1 1 1 1 1
6-9	0 0 0 0 0 0 0 0 0 0 0 0 0 0 0 0 0 0 0 0 0 0 0 0
10-11	1 1 1 1 1 1 1 1 1 1 1 1 1 1 1 1 1 1 1 1 1 1 1 1
12-19	0 0 0 0 0 0 0 0 0 0 0 0 0 0 0 0 0 0 0 0 0 0 0 0
20	1 1 1 1 1 1 1 1 1 1 1 1 1 1 1 1 1 1 1 1 1 1 1 1
21	1 1 1 1 1 1 1 1 1 1 1 1 1 1 1 1 1 1 1 1 1 1 1 0
22-24	0 0 0 0 0 0 0 0 0 0 0 0 0 0 0 0 0 0 0 0 0 0 0 0
25	0 0 0 0 0 0 0 0 0 0 1 1 1 1 1 1 1 1 1 1 1 1 1 0
26	0 0 0 0 0 0 0 0 0 0 0 0 0 0 0 0 0 0 0 0 0 0 0 0
27-29	1 1 1 1 1 1 1 1 1 1 1 1 1 1 1 1 1 1 1 1 1 1 1 1
30	0 0 0 0 0 0 0 1 1 1 1 1 1 1 1 1 1 1 1 1 1 1 1 1
31-33	0 0 0 0 0 0 0 0 0 0 0 0 0 0 0 0 0 0 0 0 0 0 0 0
34	0 0 0 0 0 0 0 1 1 1 1 1 1 1 1 1 1 1 1 1 1 1 1 1
35-36	1 1 1 1 1 1 1 1 1 1 1 1 1 1 1 1 1 1 1 1 1 1 1 1
37	0 0 0 0 0 0 0 1 1 1 1 1 1 1 1 1 1 1 1 1 1 1 1 1
38	0 0 0 0 0 0 0 0 0 0 0 0 0 0 0 0 0 0 0 0 0 0 0 0
39	0 0 0 0 0 0 0 0 0 0 0 1 1 1 1 1 1 1 1 1 1 1 1 0
40	1 1 1 1 1 1 1 1 1 1 1 1 1 1 1 1 1 1 1 1 1 1 1 1
41-42	0 0 0 0 0 0 0 0 0 0 0 0 0 0 0 0 0 0 0 0 0 0 0 0
43	1 1 1 1 1 1 1 1 1 1 1 1 1 1 1 1 1 1 1 1 1 1 1 1
44	0 0 0 0 0 0 0 0 0 0 0 0 0 0 0 0 0 0 0 0 0 0 0 0
45	1 1 1 1 1 1 1 1 1 1 1 1 1 1 1 1 1 1 1 1 1 1 1 1
46-52	0 0 0 0 0 0 0 0 0 0 0 0 0 0 0 0 0 0 0 0 0 0 0 0
53	0 0 0 0 0 0 0 1 1 1 1 1 1 1 1 1 1 1 1 1 1 1 1 1
54	0 0 0 0 0 0 0 0 0 1 1 1 1 1 1 1 1 1 1 1 1 1 1 1

Table III
The Generation Outages and Resulted Frequency Nadirs at Scheduling Hours Using the Single SFR Model (Case 2)

Time	Single SFR	
	Power Outage (Gen No) [MW]	F_{nadir} [HZ]
1	278(29)	49.483
2	256(29)	49.524
3	256(29)	49.524
4	256(29)	49.524
5	256(29)	49.524
6	256(29)	49.524
7	278(29)	49.493
8	278(29)	49.493
9	300(29)	49.478
10	**325(36)**	**49.434**
11	325(36)	49.467
12	325(36)	49.467
13	325(36)	49.467
14	325(36)	49.467
15	325(36)	49.467
16	325(36)	49.467
17	325(36)	49.467
18	325(36)	49.467
19	300(29)	49.508
20	300(29)	49.508
21	300(29)	49.508
22	300(29)	49.508
23	300(29)	49.508
24	278(29)	49.507

The generation outages, the equivalent inertia, equivalent governor droop of areas and the frequency nadirs are given in Table IV. It is noted that the equivalent inertia of each area are given in per unit at the base power of total system. The worst frequency deviations occur at hour 10. The outage of largest generating unit (i.e. 325 MW at bus 36) results in three different SFRs. The frequency responses using the single SFR and the multi-area SFR are shown in Fig. 1 at hour 10. It can be seen that there is a significant difference between the single SFR and the proposed multi-area SFR. Also, by comparing Table III and Table IV, it can be seen that there is significant difference between frequency nadirs, verifying the importance of multi-area SFR model. Another important issue in the proposed multi-area SFR is its ability to capture the local characteristics of frequency dynamics. Practically, a generation outage in a given electric area causes different nadirs in all areas. To show this issue, the largest generating unit in each area is removed and then the resulted SFRs are assessed. In IEEE 118-bus system, under the largest generation outage of each area, the frequency nadirs of the resulted system frequency responses are reported in Table IV.

According to Table III, using the single SFR model, the worst frequency nadir is 49.434 Hz that is occurred at hour 10 under the generation deficiency of 325 MW due to the outage of unit at bus 36. According to Table IV, under the same outage (i.e. fault 2), using the multi-area SFR model, the frequency nadirs at Area 1, Area 2, and Area 3 are equal to 49.395 Hz, 49.345 Hz, and 49.578 Hz, respectively. However, the worst frequency nadir is equal to 49.073 Hz as reported in Table IV. For better clarification, the frequency responses of areas using the multi-area SFR under the 325 MW generation deficiency due to the outage of generating unit at bus 40 (i.e. fault 3) is illustrated in Fig. 2. In other word, the same generation outage (e.g. 325 MW) but at different areas results in different frequency nadirs. This issue cannot be captured by a single SFR model. According to the obtained results, the generation outage in a given area cause the worst frequency nadirs in its related area.

A. FSCUC with Single SFR

In this case, the single SFR is added to the UC problem. The results of the single SFR-based FSCUC model are reported in Table V. According to Table V, it can be seen that the on/off states of generating units differ a little from Case 1 (e.g. unit 24). The total daily scheduling cost is increased to 819216.9 $ which is greater than the total cost of Case 1. Since the entire network has a single SFR, the outage of unit 45, as the largest unit, governs the system frequency response.

Table IV
The Generation Outages and Resulted Frequency Nadirs at Hour 10 Using the Multi-Area SFR Model (Case 2)

Area	Fault No	Power Outage (Gen No) [MW]	Equivalent inertia [s]	Equivalent governor droop	F_{nadir} [HZ]
1	1	255(4)	0.654	0.493	49.362
2	1	255(4)	1.52	0.108	49.522
3	1	255(4)	0.621	0.179	49.668
1	2	325(36)	0.915	0.225	49.395
2	2	325(36)	1.245	0.145	49.345
3	2	325(36)	0.621	0.179	49.578
1	3	325(40)	0.96	0.214	49.396
2	3	325(40)	1.599	0.102	49.384
3	3	325(40)	0.21	0.265	49.073

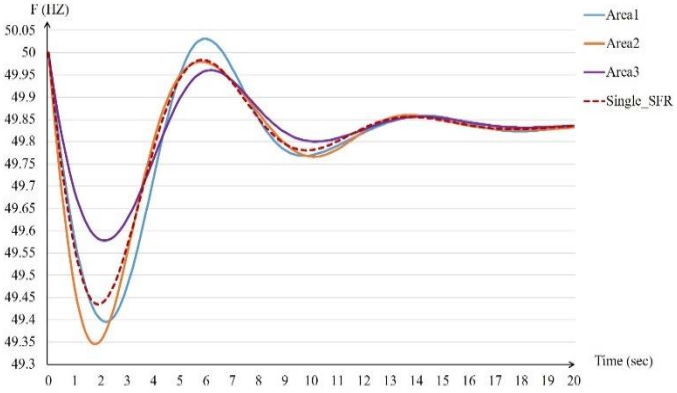

Fig. 1. Frequency responses using both single SFR and multi-area SFR under the largest outage at hour 10 (Case 2)

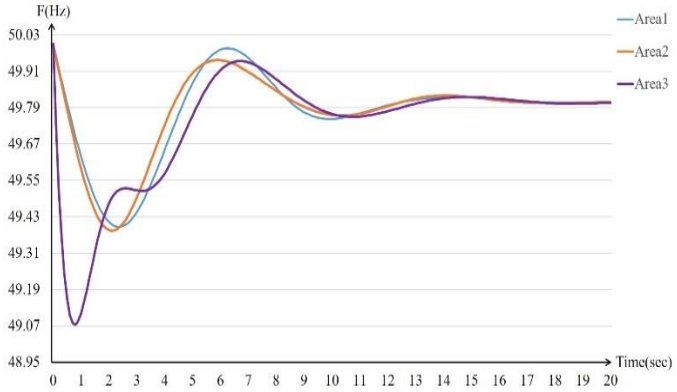

Fig. 2. Frequency responses using multi-area SFR model in areas under fault 3 and hour 10(Case 2)

Table V
The On /Off States of Generating Units in Case 2-A

Unit	Hours (1-24)
1-3	0 0 0 0 0 0 0 0 0 0 0 0 0 0 0 0 0 0 0 0 0 0 0 0
4-5	1 1 1 1 1 1 1 1 1 1 1 1 1 1 1 1 1 1 1 1 1 1 1 1
6-9	0 0 0 0 0 0 0 0 0 0 0 0 0 0 0 0 0 0 0 0 0 0 0 0
10-11	1 1 1 1 1 1 1 1 1 1 1 1 1 1 1 1 1 1 1 1 1 1 1 1
12-19	0 0 0 0 0 0 0 0 0 0 0 0 0 0 0 0 0 0 0 0 0 0 0 0
20	1 1 1 1 1 1 1 1 1 1 1 1 1 1 1 1 1 1 1 1 1 1 1 1
21	1 1 1 1 1 1 1 1 1 1 1 1 1 1 1 1 1 1 1 1 1 1 1 0
22-23	0 0 0 0 0 0 0 0 0 0 0 0 0 0 0 0 0 0 0 0 0 0 0 0
24	1 1 1 1 1 1 1 1 1 1 1 1 1 1 1 1 1 1 1 0 0 0 0 0
25	0 0 0 0 0 0 0 0 0 0 1 1 1 1 1 1 1 1 1 1 1 1 1 0
26	0 0 0 0 0 0 0 0 0 0 0 0 0 0 0 0 0 0 0 0 0 0 0 0
27-29	1 1 1 1 1 1 1 1 1 1 1 1 1 1 1 1 1 1 1 1 1 1 1 1
30	0 0 0 0 0 0 1 1 1 1 1 1 1 1 1 1 1 1 1 1 1 1 1 1
31-33	0 0 0 0 0 0 0 0 0 0 0 0 0 0 0 0 0 0 0 0 0 0 0 0
34	0 0 0 0 0 0 1 1 1 1 1 1 1 1 1 1 1 1 1 1 1 1 1 1
35-36	1 1 1 1 1 1 1 1 1 1 1 1 1 1 1 1 1 1 1 1 1 1 1 1
37	0 0 0 0 0 0 1 1 1 1 1 1 1 1 1 1 1 1 1 1 1 1 1 1
38	0 0 0 0 0 0 0 0 0 0 0 0 0 0 0 0 0 0 0 0 0 0 0 0
39	0 0 0 0 0 0 0 0 0 0 0 1 1 1 1 1 1 1 1 1 1 1 1 0
40	1 1 1 1 1 1 1 1 1 1 1 1 1 1 1 1 1 1 1 1 1 1 1 1
41-42	0 0 0 0 0 0 0 0 0 0 0 0 0 0 0 0 0 0 0 0 0 0 0 0
43	1 1 1 1 1 1 1 1 1 1 1 1 1 1 1 1 1 1 1 1 1 1 1 1
44	0 0 0 0 0 0 0 0 0 0 0 0 0 0 0 0 0 0 0 0 0 0 0 0
45	1 1 1 1 1 1 1 1 1 1 1 1 1 1 1 1 1 1 1 1 1 1 1 1
46-52	0 0 0 0 0 0 0 0 0 0 0 0 0 0 0 0 0 0 0 0 0 0 0 0
53	0 0 0 0 0 0 1 1 1 1 1 1 1 1 1 1 1 1 1 1 1 1 1 1
54	0 0 0 0 0 0 0 0 1 1 1 1 1 1 1 1 1 1 1 1 1 1 1 1

Case 3: FSCUC with Multi-Area SFR

In this case, the simulation results of the proposed FSCUC model with considering the multi-area SFR model are presented. In this case, the multi-area SFR model is included in

the UC model. It is assumed that the test system has three electric areas. These areas are assumed according to [9] and [32]. The obtained unit scheduling should be able to survive all single generation outages with maintaining the system frequency response in a safe range. In fact, the frequency stability is optimized by proper unit scheduling and reserve allocation via the related governors without considering FES. Governors and load damping are considered. The allowable frequency nadir is assumed as 49.5 Hz. The optimal unit scheduling is obtained similar to Case 1 but with different generation levels and reserve. For example, the unit scheduling at hour 10 is reported in Table VI, for this case and Case 1. In this case, the proposed FSCUC provides the frequency stability by proper reserve allocation and adjustment of largest generation outages.

The amounts of largest outages, the equivalent inertia and equal governor droop of areas using the FSCUC are reported in Table VII. Also, the amounts of largest generation outages using the network constrained UC model were reported in Table IV. By comparing Table IV and Table VII, it can be seen that the proposed FSCUC model adjusts the generation levels such that the amounts of generation outages are decreased to lower the severity of input disturbance and promoting the frequency response. Also by comparing Table IV and Table VII, it can be seen that the equivalent inertia of areas when fault occurs in that area has increased in case 3 because outages of generators 5, 27, and 43 in Case 3 results in lower inertia reduction with respect to the outages of generators 4, 36, and 40 in Case 2. Therefore, unlike Case 1, in Case 3, by proper scheduling, the frequency stability is preserved.

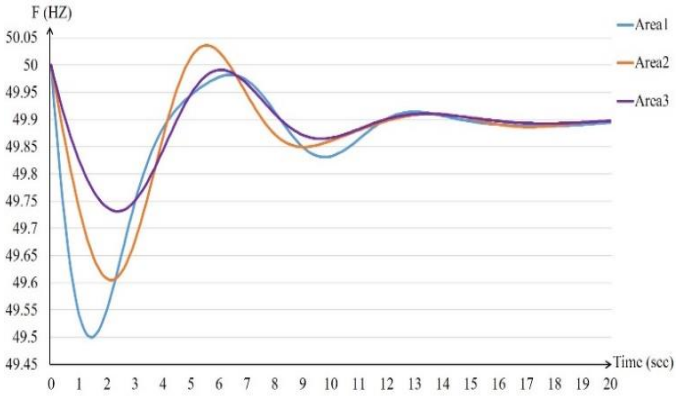

Fig. 3. Improved frequency responses using multi-area SFR (FSCUC) model in areas under fault 1 and hour 10(Case 3)

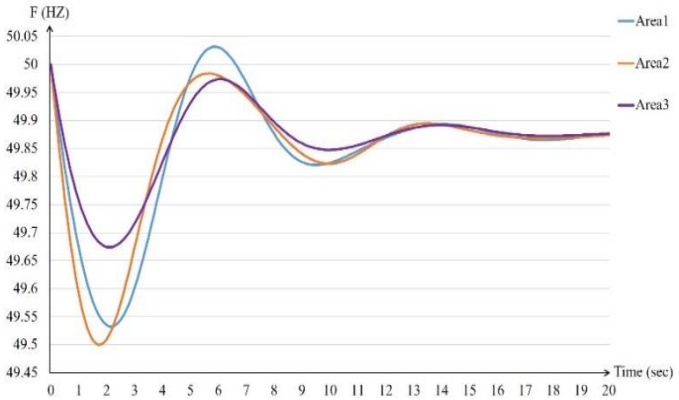

Fig. 4. Improved frequency responses using multi-area SFR (FSCUC) model in areas under fault 2 and hour 10(Case 3)

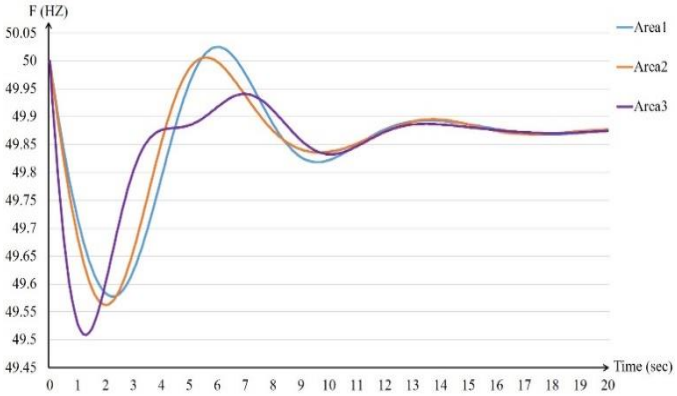

Fig. 5. Improved frequency responses using multi-area SFR (FSCUC) model in areas under fault 3 and hour 10(Case 3)

Table VI
Comparing Unit Scheduling of Case 3 and case 1

Unit	Case 1		Case 3	
	On or off	Power [MW]	On or off	Power [MW]
1-3	0	0	0	0
4	1	255	1	234.1564
5	1	199.7721	1	234.1565
6-9	0	0	0	0
10	1	220	1	229.5596
11	1	250	1	234.1564
12-19	0	0	0	0
20	1	170	1	170
21	1	110	1	130
22-26	0	0	0	0
27	1	218.1244	1	254.4402
28	1	164	1	181.5472
29	1	300	1	254.4401
30	1	80	1	80
31-33	0	0	0	0
34	1	100	1	100
35	1	100	1	100
36	1	325	1	254.4401
37	1	100	1	100
38-39	0	0	0	0
40	1	325	1	280
41-42	0	0	0	0
43	1	220	1	280.0001
44	0	0	0	0
45	1	260	1	280
46-52	0	0	0	0
53	1	100	1	100
54	1	50	1	50

Table VII
The Generation Outages and Resulted Frequency Nadirs at Hour 10 Using the Multi-Area SFR Model (Case 3)

Area	Fault No	Power outage (outage unit) [MW]	Equivalent inertia [s]	Equivalent governor droop
1	1	234.156(5)	0.736	0.251
2	1	234.156(5)	1.400	0.117
3	1	234.156(5)	0.571	0.195
1	2	254.440(27)	0.901	0.228
2	2	254.440(27)	1.248	0.136
3	2	254.440(27)	0.612	0.181
1	3	280.001(43)	0.826	0.249
2	3	280.001(43)	1.376	0.119
3	3	280.001(43)	0.556	0.198

The worst frequency responses using the proposed FSCUC model at hour 10 are illustrated in Fig. 3, Fig. 4, and Fig. 5. It can be seen that using the proposed FSCUC model, the frequency nadirs are greater than 49.5 Hz. The total operation cost of FSCUC is increased to 819560.36$ which is greater than the total cost of network constrained UC in Case 1.

Case 4: FSCUC with Flywheel

In Case 3, the frequency stability was satisfied using only the adjustment of generation levels and reserves. Also, the governor response and load damping were considered. It was shown that the FSCUC will increase the operational cost. In this case, the FES is utilized to contribute in primary frequency support. Indeed, as an energy storage device, the FES can be used for different purposes such as frequency support, reserve management, and smoothing the power output of intermittent renewable resources such as wind farms. To this end, using the proposed multi-area SFR model, the FES model is added to the FSCUC model. For each area, one FES is included. Droops of FESs at Area 1, Area 2, and Area 3 are assumed to be 0.38, 0.27, and 0.34, respectively. The FES enables the system operator, to keep the unit schedule to the most economic configuration as given in Case 1, while the frequency response is improved significantly. Using the FSCUC model and under the presence of FES, the frequency responses are obtained as illustrated in Fig. 6, Fig. 7, and Fig. 8, for Area 1, Area 2, and Area 3, respectively. Using the FES, all frequency nadirs are now greater than 49.7 Hz. Additionally, using the FES, the additional cost of unit scheduling (i.e. 1227.72$) is saved. For better clarification, the outputs of FESs are illustrated in Fig. 9. According to Fig. 9, it can be seen that at the beginning of the disturbance (i.e. generation outage), due to the severity of frequency decline, the contributions of FESs are significantly high. Such inertial response avoids the undesired frequency nadirs. By decreasing the frequency deviation, the output of FESs is decreased and after 10 seconds from the initial disturbance, the power output remains stable and for example, the FES of the Area 2 delivers 112 MW after 0.1 s.

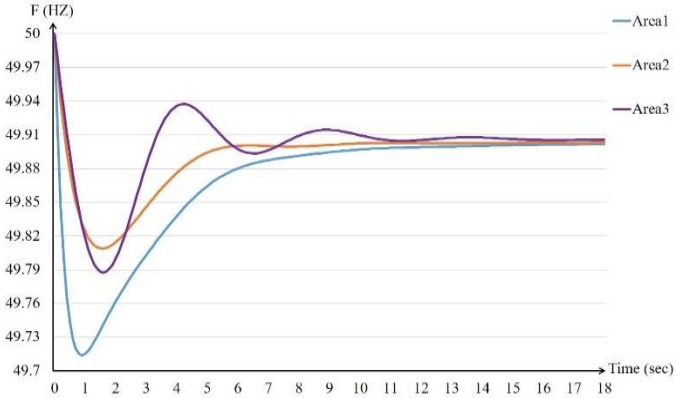

Fig. 6. Improved frequency responses using multi-area SFR (FSCUC) model in areas under fault 1 and hour 10 with flywheel (Case 4)

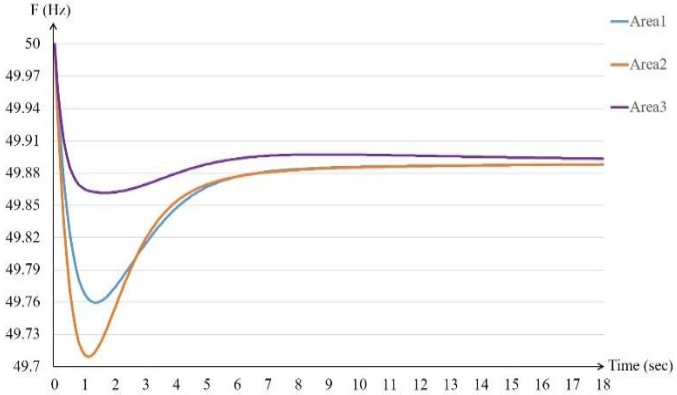

Fig. 7. Improved frequency responses using multi-area SFR (FSCUC) model in areas under fault 2 and hour 10 with flywheel (Case 4)

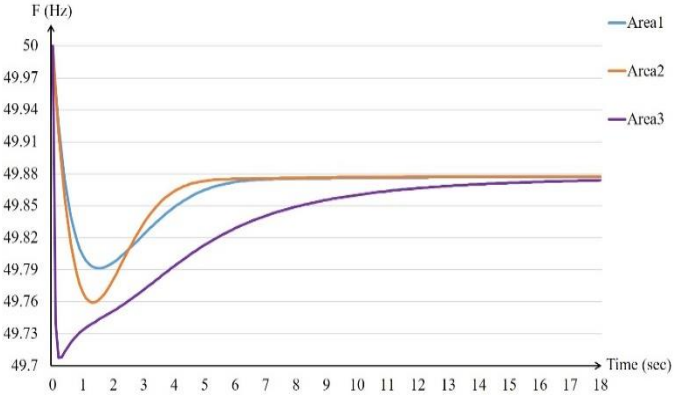

Fig. 8. Improved frequency responses using multi-area SFR (FSCUC) model in areas under fault 3 and hour 10 with flywheel (Case 4)

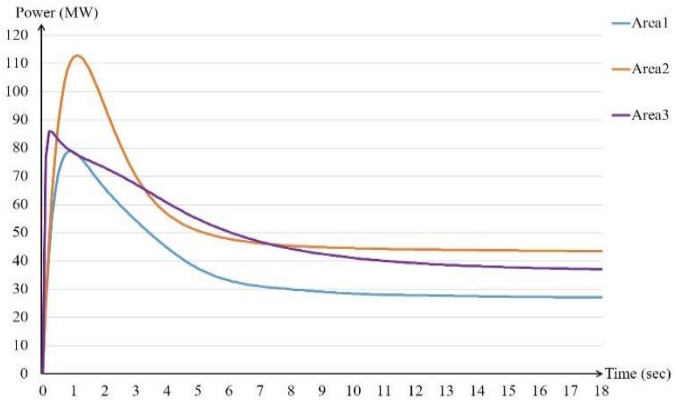

Fig. 9. Power output of flywheels in areas under fault 2 at hour 10 using the multi-area SFR (FSCUC) model

The FES costs consist of capital costs, cost of power losses, and maintenance costs. Since the proposed model is conducted in short term operational horizon, the capital cost is not included. Also, due to the daily horizon of the study, the maintenance cost is assumed negligible. New FES technologies have a very low energy loss and it is assumed that the FES has no power loss. In other words, the operation cost of FES is assumed to be negligible. This assumption is an approximation.

The CPU times of UC, FSCUC with single SFR and FSCUC with multi-area SFR are reported in Table VIII, all simulations are done using a PC with Processor: Core i7 6700HQ CPU @ 2.60GHz, and RAM 8 GB. Based on Table VIII, the CPU time of the UC model without considering any frequency stability constraint is equal to 38s. By adding the single SFR model and the proposed multi-area SFR model to the UC problem, the CPU time of the resulted FSCUC models is increased. The CPU time depends on the optimality gap of the CPLEX solver. While, the results of the UC, single SFR FSCUC and multi-area SFR FSCUC are reported using the optimality gap of 0%, 0.3% and 0.3% respectively, the CPU times have been reported in Table VIII for upper optimality gap (i.e. 1.5 %) to see the CPU time reduction. Unlike the single SFR model, the proposed multi-area SFR considers the local dynamics of the frequency variations, and therefore the computation time is increased. The amount of time step or Δt affects both the computational complexity and the accuracy of frequency response. By increasing Δt, the computational time and accuracy of the frequency response decrease and also with decreasing Δt, the computational time and accuracy of the frequency response increase. The computational time of FSCUC with single-SFR and multi-SFR FSCUC models under different values of time

step or Δt are reported in Table IX. The optimality gap is considered as 0.3%. According to Table I, using the multi-SFR FSCUC model, when the time step is increased from 0.1s to 0.2s, the Run Time is decreased from 96min to 33min & 21s. The same conclusion is true for single-SFR FSCUC model.

The proposed multi-area SFR represents each area with a unique SFR and therefore the CPU time of the resulted FSCUC increases when the number of areas is increased. The number of electric areas are not huge even in practical power systems. Also, by adjusting the optimality gap and utilizing High Performance Computing (HPC) tools the CPU time can be reduced more for large power systems.

Table VIII
Computational Times of Simulated single SFR and multi-area SFR FSCUC Models

Model	Optimality Gap	Run Time
UC	0 %	38 s
FSCUC with Single SFR	0.3 %	16 min & 31 s
	1.5 %	2 min & 48 s
FSCUC with multi-area SFR	0.3 %	96 min
	1.5 %	7 min & 16 s

Table IX
Computational Times of FSCUC Models Using Different Δt

Model	Time Step (Δt)	Run Time
FSCUC with Single SFR	0.2s	9 min & 27 s
	0.1s	16 min & 31 s
	0.05s	26 min & 33 s
FSCUC with multi-area SFR	0.2s	33 min & 21 s
	0.1s	96 min
	0.05s	270 min & 58 s

Table X
The Generation Outages and Resulted Frequency Nadirs in The Presence of Wind Farms at Hour 10 Using the Multi-Area SFR Model (Case 4-A)

Area	Fault No	Power outage (outage unit) [MW]	Equivalent inertia [s]	Equivalent governor droop
1	1	255(4)	0.364	1.160
2	1	255(4)	1.263	0.145
3	1	255(4)	0.616	0.179
1	2	325(36)	0.625	0.305
2	2	325(36)	1.002	0.224
3	2	325(36)	0.616	0.179
1	3	325(40)	0.656	0.291
2	3	325(40)	1.325	0.139
3	3	325(40)	0.204	1.265

A. Case Studies in Low Inertia Conditions

The penetration of non-synchronous renewable resources such as wind farms challenges the power system frequency stability due to inertia deterioration. In this case, generating units at buses 11, 29 and 43 are replaced with wind farms. Each generator is located at a different electric area. Therefore, the total system inertia is deteriorated. Without considering frequency stability constraints, the generation outages cause undesired frequency nadirs. Based on multi-area SFR, the FES is utilized to promote the system frequency response in UC model in such a low inertia condition. The amount of power outage and the equivalent reduced inertia are reported in Table X. The maximum deterioration in inertia occurs at area 2, since the largest wind farm is assumed at bus 29 of area 2. To this end, the system frequency responses with and without wind farms are illustrated in Fig. 10. Now, the FESs are used to improve the system frequency responses under wind penetration. The resulted SFRs are depicted in Fig. 11. It can be seen that the FES increase the frequency nadir from 49.2 Hz to 49.7 Hz. Such improvement in system frequency responses are achieved without any additional generation cost. The power output of the FES in Area 2 is shown in Fig. 12. As can been seen, the FES of area 2 needs to generate more power (i.e. 10 MW) in the presence of wind farm.

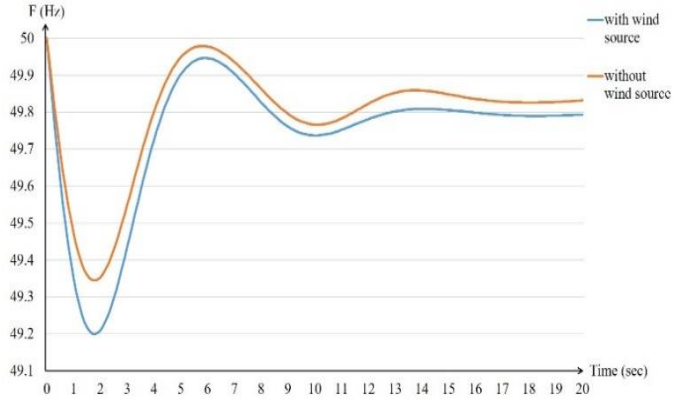

Fig. 10. Frequency response for area2 at fault 2 and time 10 with and without wind resource (Case 4-A)

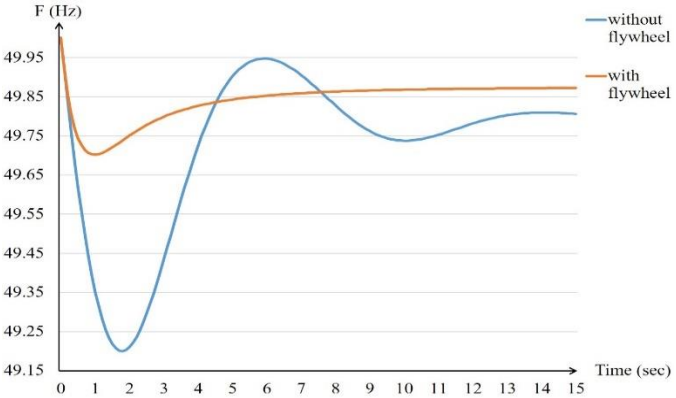

Fig. 11. Frequency response for area2 at fault 2 and time 10 with and without flywheel participation in presence of wind resource (Case 4-A)

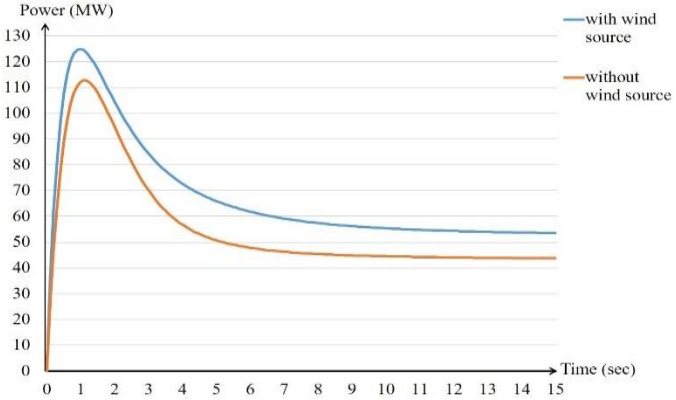

Fig. 12. Power output of flywheels in areas at time 10 with and without wind resource (Case 4-A)

IV. Conclusion

In this paper, a multi-area frequency stability constrained UC model was proposed to achieve a daily unit commitment model with considering primary frequency requirements. The power generation levels, operating reserves, and FES were optimized to support the system frequency response under generation outages. The major findings of this work can be summarized as follows. 1) Considering frequency stability constraints in UC study will guarantee the safety of system frequency response. By proper unit scheduling and reserve allocation, the system frequency response remains in a safe threshold under single outages of generating units. 2) The single SFR model acts based

on the Center-of-Inertia and assume a similar frequency variation for all buses. The single SFR model is not able to capture the local variations of frequency nadirs in a multi-area power system. 3) The proposed multi-area SFR model considers the local changes of frequency variations which is more realistic than the single SFR model. According to the proposed multi-area SFR model, the location of generation outage impacts the resulted frequency nadirs significantly. 4) The FES is a valuable source of inertial frequency support and can prevent the undesired frequency nadirs under severe generation outages. Also, the FES keeps the unit scheduling program at its economic point, while the frequency stability is preserved.

APPENDIX

In this part, the linearized equivalent of nonlinear constraints of the proposed Frequency Stability Constrained Unit Commitment (FSCUC) model are presented. All presented linearization in this part are exact without any approximation.

A. Unit commitment linearization

By utilizing binary variables respectively $(U_{i,t}, U_{i,t-1})$ for determine on or off status of generation units, the model turns into a non-linear problem. Therewith, the following linearization has been utilized for turning the problem into a MIP model. The equations iv and v are linearized forms of equations (14) and (15).

$$\varphi_{i,t} \le U_{i,t} \qquad \forall i \in \Omega_G, t \in \Omega_T \qquad \text{i}$$

$$\varphi_{i,t} \le U_{i,t-1} \qquad \forall i \in \Omega_G, t \in \Omega_T \qquad \text{ii}$$

$$\varphi_{i,t} \ge U_{i,t} + U_{i,t-1} - 1 \qquad \forall i \in \Omega_G, t \in \Omega_T \qquad \text{iii}$$

$$P^g_{i,t} - P^g_{i,t-1} \le (U_{i,t} - \varphi_{i,t}) * P_i^{min} + RU_i * (\varphi_{i,t} - U_{i,t}) \qquad \forall i \in \Omega_G, t \in \Omega_T \qquad \text{iv}$$

$$P^g_{i,t-1} - P^g_{i,t} \le (U_{i,t-1} - \varphi_{i,t}) * P_i^{min} + RD_i * (\varphi_{i,t} - U_{i,t-1}) \qquad \forall i \in \Omega_G, t \in \Omega_T \qquad \text{v}$$

B. SFR linearization

All reformulations in this part are utilized to linearize the product of binary to continuous variables that are used in constraints (35) -(38), (43) -(44) and (46). Hence, the equality constraints given by vi and vii are obtained by placing (35) -(38) and (46) with equations (43) -(44).

$$A_{v,c,t,n} = \frac{1}{2(\frac{\sum_{i\in\Omega_C^G} H_i * S_i * U^F_{v,i,t}}{\sum_{i\in\Omega_G} S_i * U^F_{v,i,t}})} * (\Delta r_{v,c,t,n} - (Fm_{v,c} * \frac{\Delta P_{c,t}}{\sum_{i\in\Omega_G} S_i * U^F_{v,i,t}}) - (\frac{\sum_{d\in\Omega_A} Tl_{c,d} * PL^{af}_{v,c,d,t,n+1}}{\sum_{i\in\Omega_G} S_i * U^F_{v,i,t}}) - (\frac{\Delta f_{v,c,t,n}}{R_c^{FL}}) - DF/3 * \Delta f_{v,c,t,n}) \quad \forall v \in \Omega_C^F, c \in \Omega_A, t \in \Omega_T, n \in \Omega_N \qquad \text{vi}$$

$$\Delta r_{v,c,t,n} = \Delta r_{v,c,t,n-1} + \frac{\Delta t}{TK} * ((-\Delta f_{v,c,t,n-1} * (\frac{\sum_{i\in\Omega_C^{Go}} \frac{S_i * U^F_{v,i,t}}{R_i}}{\sum_{i\in\Omega_G} S_i * U^F_{v,i,t}})) - \Delta r_{v,c,t,n-1}) \quad \forall v \in \Omega_C^F, c \in \Omega_A, t \in \Omega_T, n \in \Omega_N, n > 1 \qquad \text{vii}$$

By multiplying both sides of vii to the $(\sum_{i\in\Omega_G} S_i * U^F_{v,i,t})$, the following equality constraints are obtained.

$$\sum_{i\in\Omega_C^G} 2 * A_{v,c,t,n} * H_i * S_i * U^F_{v,i,t} = \sum_{i\in\Omega_G} \Delta r_{v,c,t,n} * S_i * U^F_{v,i,t} - \left(\frac{\Delta f_{v,c,t,n}}{R_c^{FL}}\right) * S_i * U^F_{v,i,t} - \frac{DF}{3} * \Delta f_{v,c,t,n} * S_i * U^F_{v,i,t} - \sum_{d\in\Omega_A} Tl_{c,d} * PL^{af}_{v,c,d,t,n+1} - \Delta P_{c,t} * Fm_{v,c} \quad \forall v \in \Omega_C^F, c \in \Omega_A, t \in \Omega_T, n \in \Omega_N \qquad \text{viii}$$

$$\sum_{i\in\Omega_C^{Go}} -\frac{\Delta t}{TK} * \Delta f_{v,c,t,n-1} * \frac{S_i * U^F_{v,i,t}}{R_i} = \sum_{i\in\Omega_G} \Delta r_{v,c,t,n} * S_i * U^F_{v,i,t} + \left(\frac{\Delta t}{TK} - 1\right) * \Delta r_{v,c,t,n-1} * S_i * U^F_{v,i,t} \quad \forall v \in \Omega_C^F, c \in \Omega_A, t \in \Omega_T, n \in \Omega_N, n > 1 \qquad \text{ix}$$

Now, by linearizing the product of the continuous and binary variables (i.e. $A_{\{*\}} * U^F_{v,i,t}$), the linearization is achieved. Finally, equations x to xxxi are linearized form of equations (35)-(38) , (43)-(44) and (46).

$$\sum_{i\in\Omega_C^G} A^b_{v,c,i,t,n} = \sum_{i\in\Omega_G} A^d_{v,c,i,t,n} - A^g_{v,c,i,t,n} - A^c_{v,c,i,t,n} - \sum_{d\in\Omega_A} Tl_{c,d} * PL^{af}_{v,c,d,t,n+1} - \Delta P_{c,t} * Fm_{v,c} \quad \forall v \in \Omega_C^F, c \in \Omega_A, t \in \Omega_T, n \in \Omega_N \qquad \text{x}$$

$$\sum_{i\in\Omega_C^{Go}} A^a_{v,c,i,t,n} = \sum_{i\in\Omega_G} \left[A^d_{v,c,i,t,n} + \left(\frac{\Delta t}{TK} - 1\right) * A^d_{v,c,i,t,n-1}\right] \quad \forall v \in \Omega_C^F, c \in \Omega_A, t \in \Omega_T, n \in \Omega_N, n > 1 \qquad \text{xi}$$

$$-M * U^F_{v,i,t} \le A^b_{v,c,i,t,n} \quad \forall v \in \Omega_C^F, c \in \Omega_A, i \in \Omega_C^G, t \in \Omega_T, n \in \Omega_N \qquad \text{xii}$$

$$A^b_{v,c,i,t,n} \le M * U^F_{v,i,t} \quad \forall v \in \Omega_C^F, c \in \Omega_A, i \in \Omega_C^G, t \in \Omega_T, n \in \Omega_N \qquad \text{xiii}$$

$$-M * (1 - U^F_{v,i,t}) \le A^b_{v,c,i,t,n} - (2 * A_{v,c,t,n} * S_i * H_i) \quad \forall v \in \Omega_C^F, c \in \Omega_A, i \in \Omega_C^G, t \in \Omega_T, n \in \Omega_N \qquad \text{xiv}$$

$$A^b_{v,c,i,t,n} - (2 * A_{v,c,t,n} * S_i * H_i) \le M * (1 - U^F_{v,i,t}) \quad \forall v \in \Omega_C^F, c \in \Omega_A, i \in \Omega_C^G, t \in \Omega_T, n \in \Omega_N \qquad \text{xv}$$

$$-M * U^F_{v,i,t} \le A^c_{v,c,i,t,n} \quad \forall v \in \Omega_C^F, c \in \Omega_A, i \in \Omega_G, t \in \Omega_T, n \in \Omega_N \qquad \text{xvi}$$

$$A^c_{v,c,i,t,n} \le M * U^F_{v,i,t} \quad \forall v \in \Omega_C^F, c \in \Omega_A, i \in \Omega_G, t \in \Omega_T, n \in \Omega_N \qquad \text{xvii}$$

$$-M * (1 - U^F_{v,i,t}) \le A^c_{v,c,i,t,n} - ((DF/3) * \Delta f_{v,c,t,n} * S_i) \quad \forall v \in \Omega_C^F, c \in \Omega_A, i \in \Omega_G, t \in \Omega_T, n \in \Omega_N \qquad \text{xviii}$$

$$A^c_{v,c,i,t,n} - ((DF/3) * \Delta f_{v,c,t,n} * S_i) \le M * (1 - U^F_{v,i,t}) \quad \forall v \in \Omega_C^F, c \in \Omega_A. i \in \Omega_G, t \in \Omega_T, n \in \Omega_N \qquad \text{xix}$$

$$-M * U^F_{v,i,t} \le A^d_{v,c,i,t,n} \quad \forall v \in \Omega_C^F, c \in \Omega_A, i \in \Omega_G, t \in \Omega_T, n \in \Omega_N \qquad \text{xx}$$

$$A^d_{v,c,i,t,n} \le M * U^F_{v,i,t} \quad \forall v \in \Omega_C^F, c \in \Omega_A, i \in \Omega_G, t \in \Omega_T, n \in \Omega_N \qquad \text{xxi}$$

$$-M * (1 - U^F_{v,i,t}) \le A^d_{v,c,i,t,n} - (\Delta r_{v,c,t,n} * S_i) \quad ,\forall v \in \Omega_C^F, c \in \Omega_A, i \in \Omega_G, t \in \Omega_T, n \in \Omega_N \qquad \text{xxii}$$

$$A^d_{v,c,i,t,n} - (\Delta r_{v,c,t,n} * S_i) \le M * (1 - U^F_{v,i,t}) \quad \forall v \in \Omega_C^F, c \in \Omega_A, i \in \Omega_G, t \in \Omega_T, n \in \Omega_N \qquad \text{xxiii}$$

$$-M * U^F_{v,i,t} \le A^a_{v,c,i,t,n} \quad \forall v \in \Omega_C^F, c \in \Omega_A, i \in \Omega_C^G, t \in \Omega_T, n \in \Omega_N, n > 1 \qquad \text{xxiv}$$

$$A^a_{v,c,i,t,n} \le M * U^F_{v,i,t} \quad \forall v \in \Omega_C^F, c \in \Omega_A, i \in \Omega_C^G, t \in \Omega_T, n \in \Omega_N, n > 1 \qquad \text{xxv}$$

$$-M * (1 - U^F_{v,i,t}) \le A^a_{v,c,i,t,n} - (-(\left(\frac{\Delta t}{TK}\right) * \Delta f_{v,c,t,n-1} * S_i)/R_i) \quad \forall v \in \Omega_C^F, c \in \Omega_A, i \in \Omega_C^G, t \in \Omega_T, n \in \Omega_N, n > 1 \qquad \text{xxvi}$$

$$A^a_{v,c,i,t,n} - (-(\left(\frac{\Delta t}{TK}\right) * \Delta f_{v,c,t,n-1} * S_i)/R_i) \le M * (1 - U^F_{v,i,t}) \quad \forall v \in \Omega_C^F, c \in \Omega_A, i \in \Omega_C^G, t \in \Omega_T, n \in \Omega_N, n > 1 \qquad \text{xxvii}$$

$$-M * U^F_{v,i,t} \le A^g_{v,c,i,t,n} \quad \forall v \in \Omega_C^F, c \in \Omega_A, i \in \Omega_G, t \in \Omega_T, n \in \Omega_N, n > 1 \qquad \text{xxviii}$$

$$A^g_{v,c,i,t,n} \le M * U^F_{v,i,t} \quad \forall v \in \Omega_C^F, c \in \Omega_A, i \in \Omega_G, t \in \Omega_T, n \in \Omega_N, n > 1 \qquad \text{xxix}$$

$$-M * (1 - U^F_{v,i,t}) \le A^g_{v,c,i,t,n} - ((\Delta f_{v,c,t,n-1}/R_c^{FL}) * S_i) \quad \forall v \in \Omega_C^F, c \in \Omega_A, i \in \Omega_G, t \in \Omega_T, n \in \Omega_N, n > 1 \qquad \text{xxx}$$

$$A^g_{v,c,i,t,n} - ((\Delta f_{v,c,t,n-1}/R_c^{FL}) * S_i) \le M * (1 - U^F_{v,i,t}) \quad \forall v \in \Omega_C^F, c \in \Omega_A, i \in \Omega_G, t \in \Omega_T, n \in \Omega_N, n > 1 \qquad \text{xxxi}$$

C. Quasi steady state SFR linearization

All the reformulations of this part are presented to exactly linearize the product of binary to continuous variables. By substituting (35) and (38) in (48), the equality constraint of xxxii is obtained. The equality constraint given in xxxii can be

rewritten as xxxiii.

$$\Delta f_{v,t}^{ss} = -\frac{Fm_{v,c} * \frac{\Delta P_{c,t}}{\sum_{i\in\Omega_G} S_i * U_{v,i,t}^F}}{DF + \frac{\sum_{i\in\Omega_C^{Go}} \frac{S_i * U_{v,i,t}^F}{R_i}}{\sum_{i\in\Omega_G} S_i * U_{v,i,t}^F}} \quad \text{xxxii}$$

$$\forall\, v \in \Omega_C^F, c \in \Omega_A, c = v, t \in \Omega_T$$

$$\Delta P_{c,t} * Fm_{v,c} + DF * \sum_{i\in\Omega_C^G} \Delta f_{v,t}^{ss} * S_i * U_{v,i,t}^F = -\sum_{i\in\Omega_C^{Go}} \Delta f_{v,t}^{ss} * \frac{S_i * U_{v,i,t}^F}{R_i} \quad \text{xxxiii}$$

$$\forall\, v \in \Omega_C^F, c \in \Omega_A, c = v, t \in \Omega_T$$

Now, by linearizing the product of the continuous and binary variables (i.e. $A_{\{*\}} * U_{v,i,t}^F$), the linearization is achieved. Finally, equations xxxiv to xlii are linearized form of equation (48).

$$\Delta P_{c,t} * Fm_{v,c} + DF * \sum_{i\in\Omega_C^G} A_{v,i,t}^e = -\sum_{i\in\Omega_C^{Go}} A_{v,i,t}^f \quad \text{xxxiv}$$

$$\forall\, v \in \Omega_C^F, c \in \Omega_A, c = v, t \in \Omega_T$$

$$-M * U_{v,i,t}^F \le A_{v,i,t}^e \qquad \forall v \in \Omega_C^F, i \in \Omega_C^G, t \in \Omega_T \quad \text{xxxv}$$

$$A_{v,i,t}^e \le M * U_{v,i,t}^F \qquad \forall v \in \Omega_C^F, i \in \Omega_C^G, t \in \Omega_T \quad \text{xxxvi}$$

$$-M * \left(1 - U_{v,i,t}^F\right) \le A_{v,i,t}^e - (\Delta f_{v,t}^{ss} * S_i) \qquad \forall v \in \Omega_C^F, i \in \Omega_C^G, t \in \Omega_T \quad \text{xxxvii}$$

$$A_{v,i,t}^e - (\Delta f_{v,t}^{ss} * S_i) \le M * \left(1 - U_{v,i,t}^F\right) \qquad \forall v \in \Omega_C^F, i \in \Omega_C^G, t \in \Omega_T \quad \text{xxxviii}$$

$$-M * U_{v,i,t}^F \le A_{v,i,t}^f \qquad \forall v \in \Omega_C^F, i \in \Omega_C^G, t \in \Omega_T \quad \text{xxxix}$$

$$A_{v,i,t}^f \le M * U_{v,i,t}^F \qquad \forall v \in \Omega_C^F, i \in \Omega_C^G, t \in \Omega_T \quad \text{xl}$$

$$-M * \left(1 - U_{v,i,t}^F\right) \le A_{v,i,t}^f - ((\Delta f_{v,t}^{ss} * S_i)/R_i) \qquad \forall v \in \Omega_C^F, i \in \Omega_C^G, t \in \Omega_T \quad \text{xli}$$

$$A_{v,i,t}^f - ((\Delta f_{v,t}^{ss} * S_i)/R_i) \le M * \left(1 - U_{v,i,t}^F\right) \qquad \forall v \in \Omega_C^F, i \in \Omega_C^G, t \in \Omega_T \quad \text{xlii}$$

V. References

[1] Y. Fu, M. Shahidehpour, and Z. Li, "Security-constrained unit commitment with AC constraints," *IEEE transactions on power systems*, vol. 20, no. 3, pp. 1538-1550, 2005.

[2] F. Bavafa, T. Niknam, R. Azizipanah-Abarghooee and V. Terzija, "A New Biobjective Probabilistic Risk-Based Wind-Thermal Unit Commitment Using Heuristic Techniques," in IEEE Transactions on Industrial Informatics, vol. 13, no. 1, pp. 115-124, Feb. 2017.

[3] Y. Xu, Z. Y. Dong, R. Zhang, Y. Xue and D. J. Hill, "A Decomposition-Based Practical Approach to Transient Stability-Constrained Unit Commitment," in *IEEE Transactions on Power Systems*, vol. 30, no. 3, pp. 1455-1464, May 2015, doi: 10.1109/TPWRS.2014.2350476.

[4] Q. Jiang, B. Zhou and M. Zhang, "Parallel augment Lagrangian relaxation method for transient stability constrained unit commitment," in *IEEE Transactions on Power Systems*, vol. 28, no. 2, pp. 1140-1148, May 2013, doi: 10.1109/TPWRS.2012.2216553.

[5] Saberi, Hossein, Turaj Amraee, Cuo Zhang, and Zhao Yang Dong. "A benders-decomposition-based transient-stability-constrained unit scheduling model utilizing cutset energy function method." *International Journal of Electrical Power & Energy Systems* 124: 106338.

[6] D. Cai, E. Mallada and A. Wierman, "Distributed Optimization Decomposition for Joint Economic Dispatch and Frequency Regulation," in *IEEE Transactions on Power Systems*, vol. 32, no. 6, pp. 4370-4385, Nov. 2017, doi: 10.1109/TPWRS.2017.2682235.

[7] Y. Jia, K. Meng, K. Wu, C. Sun and Z. Y. Dong, "Optimal Load Frequency Control for Networked Power Systems Based on Distributed Economic MPC," in *IEEE Transactions on Systems, Man, and Cybernetics: Systems*, doi: 10.1109/TSMC.2020.3019444.

[8] X. Zhao, H. n. Wei, J. Qi, P. Li and X. Bai, "Frequency Stability Constrained Optimal Power Flow Incorporating Differential Algebraic Equations of Governor Dynamics," in *IEEE Transactions on Power Systems*, doi: 10.1109/TPWRS.2020.3025335.

[9] Naghdalian, Salar, Turaj Amraee, Sadegh Kamali, and Florin Capitanescu. "Stochastic Network Constrained Unit Commitment to Determine Flexible Ramp Reserve for Handling Wind Power and Demand Uncertainties." *IEEE Transactions on Industrial Informatics* (2019).

[10] Morales-España, Germán, Ross Baldick, Javier García-González, and Andres Ramos. "Power-capacity and ramp-capability reserves for wind integration in power-based UC." *IEEE Transactions on Sustainable Energy* 7, no. 2 (2015): 614-624.

[11] G. Zhang, E. Ela and Q. Wang, "Market Scheduling and Pricing for Primary and Secondary Frequency Reserve," in *IEEE Transactions on Power Systems*, vol. 34, no. 4, pp. 2914-2924, July 2019, doi: 10.1109/TPWRS.2018.2889067.

[12] R. Ghorani, F. Pourahmadi, M. Moeini-Aghtaie, M. Fotuhi-Firuzabad and M. Shahidehpour, "Risk-Based Networked-Constrained Unit Commitment Considering Correlated Power System Uncertainties," in IEEE Transactions on Smart Grid, vol. 11, no. 2, pp. 1781-1791, 2020

[13] Prakash, Vivek, Kailash Chand Sharma, Rohit Bhakar, Har Pal Tiwari, and Furong Li. "Frequency response constrained modified interval scheduling under wind uncertainty." *IEEE Transactions on Sustainable Energy* 9, no. 1 (2017): 302-310.

[14] Teng, Fei, Vincenzo Trovato, and Goran Strbac. "Stochastic scheduling with inertia-dependent fast frequency response requirements." *IEEE Transactions on Power Systems* 31, no. 2 (2015): 1557-1566.

[15] Ahmadi, Hamed, and Hassan Ghasemi. "Security-constrained unit commitment with linearized system frequency limit constraints." *IEEE Transactions on Power Systems* 29, no. 4 (2014): 1536-1545.

[16] Anderson, Philip M., and Mahmood Mirheydar. "A low-order system frequency response model." *IEEE Transactions on Power Systems* 5, no. 3 (1990): 720-729.

[17] Restrepo, José F., and Francisco D. Galiana. "Unit commitment with primary frequency regulation constraints." *IEEE Transactions on Power Systems* 20, no. 4 (2005): 1836-1842.

[18] Badesa, Luis, Fei Teng, and Goran Strbac. "Simultaneous Scheduling of Multiple Frequency Services in Stochastic Unit Commitment." *IEEE Transactions on Power Systems* (2019).

[19] M. Malekpour, M. Zare, R. Azizipanah-Abarghooee and V. Terzija, "Stochastic frequency constrained unit commitment incorporating virtual inertial response from variable speed wind turbines," in *IET Generation, Transmission & Distribution*, vol. 14, no. 22, pp. 5193-5201, 13 11 2020, doi: 10.1049/iet-gtd.2020.0381.

[20] Z. Chu, U. Markovic, G. Hug and F. Teng, "Towards Optimal System Scheduling with Synthetic Inertia Provision from Wind Turbines," in *IEEE Transactions on Power Systems*, vol. 35, no. 5, pp. 4056-4066, Sept. 2020, doi: 10.1109/TPWRS.2020.2985843.

[21] Z. Zhang, E. Du, F. Teng, N. Zhang and C. Kang, "Modeling Frequency Dynamics in Unit Commitment with a High Share of Renewable Energy," in *IEEE Transactions on Power Systems*, vol. 35, no. 6, pp. 4383-4395, Nov. 2020, doi: 10.1109/TPWRS.2020.2996821.

[22] Wen, Yunfeng, Chuangxin Guo, Hrvoje Pandžić, and Daniel S. Kirschen. "Enhanced security-constrained unit commitment with emerging utility-scale energy storage." *IEEE Transactions on power Systems* 31, no. 1 (2015): 652-662.

[23] Delille, Gauthier, Bruno Francois, and Gilles Malarange. "Dynamic frequency control support by energy storage to reduce the impact of wind and solar generation on isolated power system's inertia." *IEEE Transactions on sustainable energy* 3, no. 4 (2012): 931-939.

[24] Wen, Yunfeng, Wenyuan Li, Gang Huang, and Xuan Liu. "Frequency dynamics constrained unit commitment with battery energy storage." *IEEE Transactions on Power Systems* 31, no. 6 (2016): 5115-5125.

[25] Silva-Saravia, Horacio, Hector Pulgar-Painemal, and Juan Manuel Mauricio. "Flywheel energy storage model, control and location for improving stability: The Chilean case." *IEEE Transactions on Power Systems* 32, no. 4 (2016): 3111-3119.

[26] Peralta, Dario, Claudio Cañizares, and Kankar Bhattacharya. "Practical Modeling of Flywheel Energy Storage for Primary Frequency Control in Power Grids." In *2018 IEEE Power & Energy Society General Meeting (PESGM)*, pp. 1-5. IEEE, 2018.

[27] Vidyanandan, K. V., and Nilanjan Senroy. "Frequency regulation in a wind–diesel powered microgrid using flywheels and fuel cells." *IET Generation, Transmission & Distribution* 10, no. 3 (2016): 780-788.

[28] Atakan, Semih, Guglielmo Lulli, and Suvrajeet Sen. "A state transition MIP formulation for the unit commitment problem." *IEEE Transactions on Power Systems* 33, no. 1 (2017): 736-748.

[29] Sun, Yingyun, Zuyi Li, Mohammad Shahidehpour, and Bo Ai. "Battery-based energy storage transportation for enhancing power system economics and security." *IEEE Transactions on Smart Grid* 6, no. 5 (2015): 2395-2402.

[30] https://spectrum.ieee.org/energy/fossil-fuels/flywheels-get-their-spin-back-with-beacon-powers-rebound

[31] https://github.com/anyacastillo/ucacopf/blob/master/118_ucacopf.dat.

[32] "Files: "JEAS_IEEE118.doc" and "IEEE118bus_figure.pdf". [Online]. Available: http://motor.ece.iit.edu/data."

[33] https://www.kios.ucy.ac.cy/testsystems/index.php/dynamic-ieee-test-systems/ieee-118-bus-modified-test-system